Korean J. Chem. Eng., 40(5), 1071-1076 (2023)
DOI: 10.1007/s11814-022-1325-7

pISSN: 0256-1115
eISSN: 1975-7220

N-doped mesoporous activated carbon derived from protein-rich biomass for energy storage applications

Kue-Ho Kim, Yun-Jae Song, and Hyo-Jin Ahn†

Department of Materials Science and Engineering, Seoul National University of Science and Technology, Seoul 01811, Korea
(*Received 15 September 2022 • Revised 12 October 2022 • Accepted 26 October 2022*)

Abstract−Biomass-derived activated carbon has attracted global attention for supercapacitor applications owing to the limitations of depletable resources and the high cost of conventional activated carbon manufacturing processes. Activated carbon for energy storage requires a large surface area for performing a high energy density, which is the main challenge for biomass-derived activated carbon. Here, we suggest a protein-rich mealworm as a competitive raw material for the activated carbon manufacturing process. Mealworm-based N-doped mesoporous carbon was developed through the synergistic effect of intrinsic amino acids and fatty acids in the mealworm and a KOH activation process. The mealworm-based N-doped mesoporous carbon electrode exhibited a competitive specific capacity at both low and high current densities (154.8 F/g at a current density of 0.2 A/g and 137 F/g at a current density of 5.0 A/g) owing to the high specific surface area (2,470.5 m^2/g) and N-doped carbon structure. This superior energy storage capability contributed to its optimized mesoporous morphology and an N-doped carbon structure, which was generated during the KOH activation process.

Keywords: Supercapacitors, Structure Engineering, Mesoporous Carbon, Doped Carbon, Biomass

INTRODUCTION

With the rising demand for energy consumption in our daily life, energy storage and utilization technologies and sustainable energy resources have attracted global attention rapidly [1-3]. Moreover, owing to environmental pollution and exhaustion of fossil fuels, governments and markets have gradually increased the proportion of renewable energy sources. Devices which are operated by electrochemical reactions, including electrochemical capacitors (ECs), fuel cells (FCs), and batteries, have received considerable attention owing to their high energy-storage performance, affordability, and eco-friendliness [4,5]. Among various electrochemical energy storage devices, ECs have notable advantages, including fast charge/discharge kinetics, high cycle stability, and excellent power density. In general, the research areas of ECs can be classified by their charge/discharge reaction types. Among them, electrical double-layer capacitors (EDLCs) store energy by physical adsorption and desorption of charged ions, which are transported by electrostatic forces, inducing non-Faradaic reaction processes [6]. On the other hand, pseudocapacitors utilize the surface redox reactions (faradaic reactions) of electrode materials according to the applied voltage. Thus, EDLCs can offer much faster charge/discharge kinetics for longer cycles than PCs. However, owing to the reaction mechanism of EDLCs, they often face the limitation of low energy density. Activated carbon is a conventional electrode material for EDLCs that is currently manufactured from depletable resources (i.e., pitches, cokes, and coals). Recently, to overcome this obstacle, biomass-derived activated carbon materials were proposed, which have various advantages such as abundant and diverse raw materials, rich oxygen- and nitrogen-containing functional groups, low cost, and eco-friendliness [7-10]. The reported raw biomass materials for activated carbon synthesis have advantages such as high abundances, simple fabrication processes, large specific surface areas, diverse functional groups, and elementary composition [11-13]. Generally, crops, fruit seeds, and plants are utilized as raw biomass materials owing to their low cost, accessibility, and large specific surface area [14-16].

Mealworms, which are the caterpillar state of *Tenebrio molitor*, are typically 2-3.5 cm in length. Owing to the advantages of rearing and storing with relatively large size, mealworms have been studied in the fields of biochemistry, evolution, biology, and immunology. Moreover, mealworms are often used as feed and pet food for birds, fish, reptiles, and arthropods owing to their high protein content, including leucine, alanine, glutamic acid, and aspartic acid. Recently, mealworms have been adopted as an edible food with high nutritional value, and the European Union (EU) has authorized mealworms as a safe food for human consumption, which passed the European Food Safety Authority in June 2021 [17]. Protein-rich mealworm compositions intrinsically contain nitrogen atoms within their molecular structures, which can form N-doped carbon structures during carbonization. Since doping is considered a powerful method for enhancing the specific capacity, the intrinsically protein-rich mealworm is potentially beneficial for supercapacitor applications [18-20]. However, the utilization of mealworms or any other insects as base materials of the carbon activation manufacturing process has not yet been reported.

In this study, we first suggest dried mealworm as a sustainable base material for the carbon activation manufacturing process. The

†To whom correspondence should be addressed.
E-mail: hjahn@seoultech.ac.kr
‡K.-H. Kim and Y.-J. Song contributed equally to this work.

N-doped mesoporous carbon structure was successfully developed using the protein (amino acid) and fat (fatty acid) from the mealworm, which acted as an N-doping source and mesopore generation agent, respectively. Moreover, by adopting the activation process with KOH, the specific surface area was maximized through carbon-consuming reactions of potassium oxide and water molecules. The N-doped mesoporous carbon derived from mealworms demonstrated better electrochemical performance than that of commercial activated carbon samples.

EXPERIMENTAL DETAILS

N-doped mesoporous activated carbon was successfully synthesized through KOH activation using protein-rich, dried mealworms as a raw material. First, the dried mealworms (OmO Co., Korea) were used after being stabilized at 400 °C in a box furnace. After heat treatment, the stabilized powder was washed using nitric acid and deionized water to remove impurities. For KOH activation, the prepared powder was poured into a KOH solution (85.0%, Samchun) and dried for 12 h to form a solid precipitate. The weight ratio of the sample to KOH was fixed at 1 : 4. All solid precipitates were carbonized at 800 °C for 2 h using N_2 gas. The carbonized powder was washed by HCl (35%, Samchun) for eliminating reactant residue during the activation process. For comparison, commercial activated carbon (YP-50f, Gelon) and bare mealworm-derived carbon samples without KOH activation were also prepared (hereafter referred to as commercial activated carbon (CAC) and carbon derived from mealworm (CM)). The KOH-activated sample is referred to as mesoporous activated carbon using mealworm base material (MACM).

The surface morphology was investigated by scanning electron microscopy (SEM; Hitachi SU8010). The structural properties and atomic bonding states were studied using high-resolution X-ray diffractometry (XRD; PANalyticalX'Pert Pro MPD) and X-ray photoelectron spectroscopy (XPS; K-ALPHA$^+$), respectively, at the Center for Research Facilities at Chonnam National University. The porous surface structure was investigated by the Brunauer-Emmett-Teller (BET) method. To evaluate the energy-storage performance of all the samples, respective active material (CAC, CM, and MACM), binder (polyvinylidene fluoride), and conductive material (ketjen black) were homogeneously mixed (7 : 2 : 1 mass ratio) with N-methyl-2-pyrrolidone (NMP; 99.5%, Aldrich) to prepare the paste. The prepared pastes were coated on Ni foam to fabricate the electrodes. The electrochemical characteristics of the electrodes was evaluated by a two-electrode measurement system consisting of a beaker-type symmetric supercapacitor cell equipped with the two prepared electrodes and 6 M KOH as the electrolyte.

RESULTS AND DISCUSSION

An N-doped mesoporous activated carbon structure was successfully prepared by adopting a protein-rich mealworm raw material and the KOH activation process (MACM). Fig. 1 shows a fabrication process image, including stabilization of the sample and subsequent KOH activation. Dried mealworms were purchased from OmO Co. (Korea) and used directly as a carbon source without any further treatment or purification. After stabilization, the mealworm powder was cleaned with nitric acid and deionized water to remove impurities, such as phosphorus pentoxide and iron oxide. During stabilization, the intrinsic amino acids (glutamic acid, aspartic acid, etc.) and fatty acids (oleic acid, linoleic acid, etc.) of protein-rich mealworms decomposed at ≈300 °C, which provided a nitrogen doping source and a slightly mesoporous structure. KOH activation was then performed to induce a carbon-consuming reaction and obtain a sufficient specific surface area (Eq. (1)-(3)):

$$2KOH \rightarrow K_2O + H_2O \quad (1)$$

$$K_2O + C \rightarrow CO + 2K \quad (2)$$

$$H_2O + C \rightarrow CO + H_2 \quad (3)$$

The KOH activation process is accompanied by the decomposition of potassium hydroxide to potassium oxide and water molecules, which react with carbon and induce the evaporation of carbon atoms as carbon oxide vapor. N-doped carbon with highly meso-

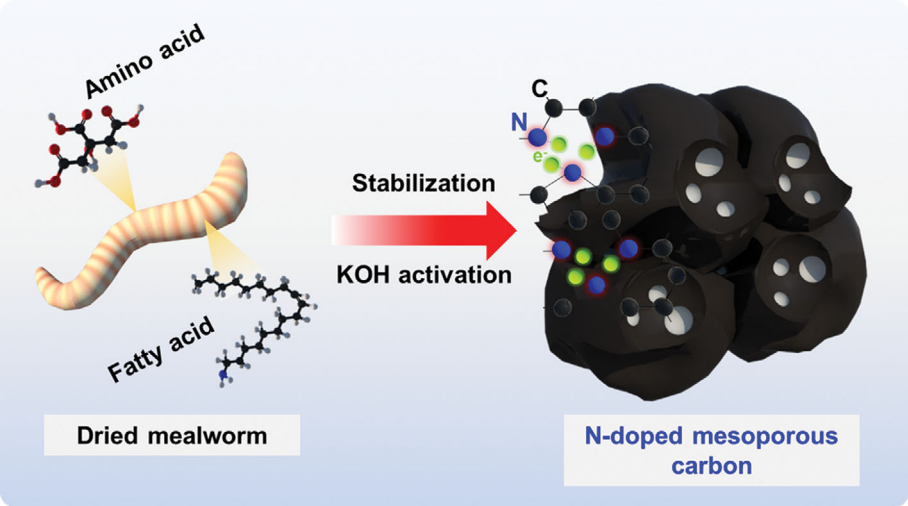

Fig. 1. Fabrication process of MACM, including stabilization of the sample and subsequent KOH activation.

porous structures were prepared through the above-mentioned reactions (~12% of activation carbon yield).

Fig. 2(a), (b), and (c) display digital photos of dried mealworm, stabilized mealworm, and MACM samples, respectively. As a raw material of activated carbon, the dried mealworms are 2.5-3.5 cm long and turn into black powder following stabilization and KOH activation. Fig. 2(d), (e), and (f) show FESEM images of the CAC, CM, and MACM samples, respectively. As can be seen, all samples appear to have a block-like, angled particle morphology. In particular, CAC possesses a bulk carbon structure with a smooth surface,

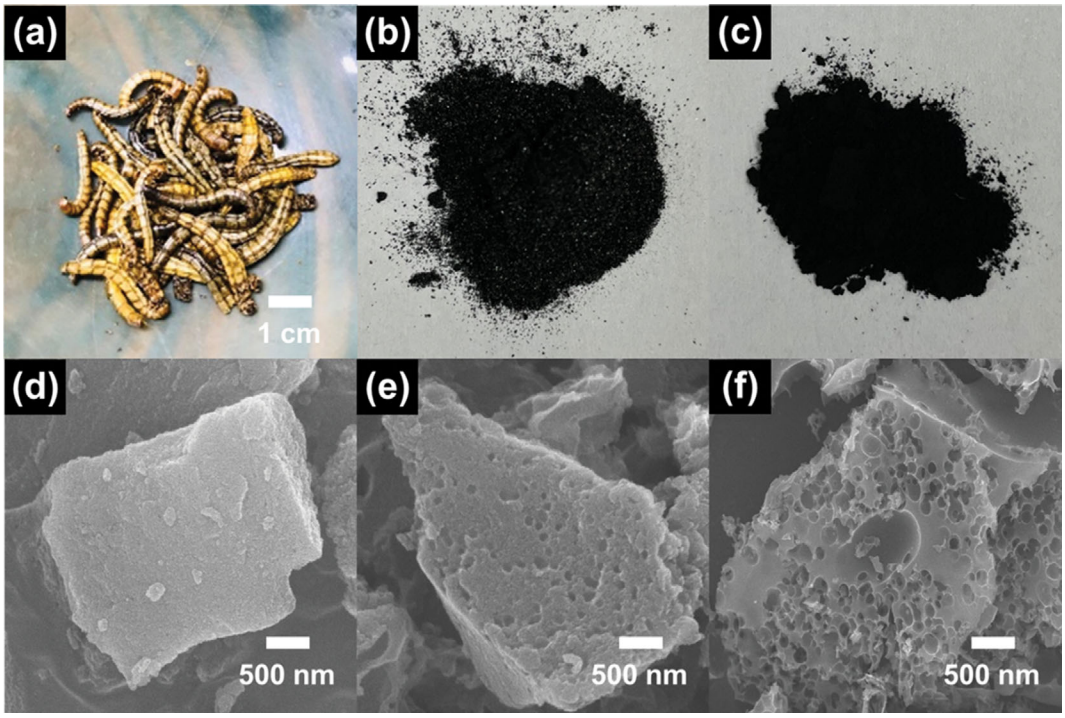

Fig. 2. Digital photos of (a) dried mealworm, (b) stabilized mealworm, and (c) MACM samples with FESEM images of the (d) CAC, (e) CM, and (f) MACM samples.

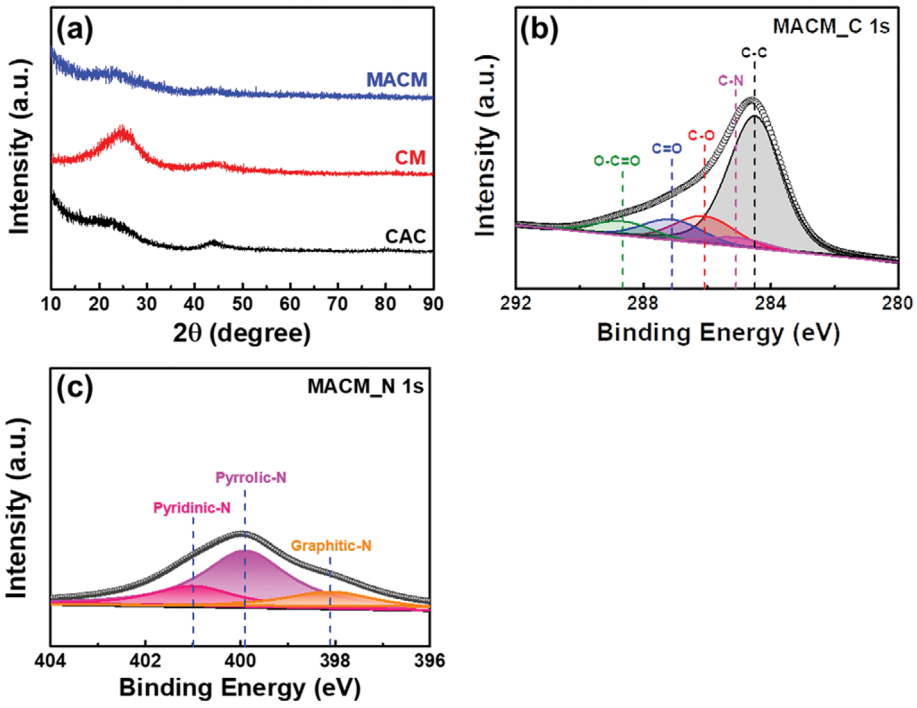

Fig. 3. (a) XRD data of all the samples and XPS spectra of (b) C 1s and (c) N 1s for MACM sample.

which is in contrast to the surface morphology of CM, with its generated mesopores. Owing to the decomposition of amino acids and fatty acids within mealworms during heat treatment, a slightly mesoporous surface morphology developed. Interestingly, MACM possesses an optimized mesoporous structure, with a larger mesopore volume fraction (32.5%) than that of CAC (19.2%) and CM (25.2%), which is caused by the KOH activation effect and mealworm raw materials. By adopting the KOH activation process, the mesoporous structure was maximized, providing high specific surface area and high ion-diffusion kinetics [21].

Fig. 3(a) presents the XRD data of all the samples, which was obtained to identify the crystal structures. All samples gave rise to amorphous diffraction peaks at ≈25.0°, corresponding to the (002) plane of graphite, which was present owing to the relatively low carbonization temperature [22]. In particular, the CAC and MACM samples exhibit weak diffraction peaks owing to their high surface area. Moreover, XPS analyses of the MACM sample were conducted to measure the atomic bonding statements in detail. The binding energy was standardized with C-C (284.5 eV) reference bonding. Fig. 3(b) displays the C 1s XPS spectra of MACM, comprising five peaks at approximately 284.5, 285.1, 286.1, 287.1, and 288.6 eV, signifying the C-C, C-N, C-O, C=O, and O-C=O bonds, respectively [23]. Notably, nitrogen bonding with carbon was confirmed, which implies that the N-doped carbon structure was successfully established through the decomposition of amino acids. The N-doped carbon structure was also confirmed by the N 1s XPS spectra of MACM, which contained the three peaks characteristic of graphitic-N, pyrrolic-N, and pyridinic-N bonds at approximately 398.2, 399.9, and 401.1 eV, respectively (see Fig. 3(c)). Nitrogen doping of the carbon structure increases the electrical conductivity by

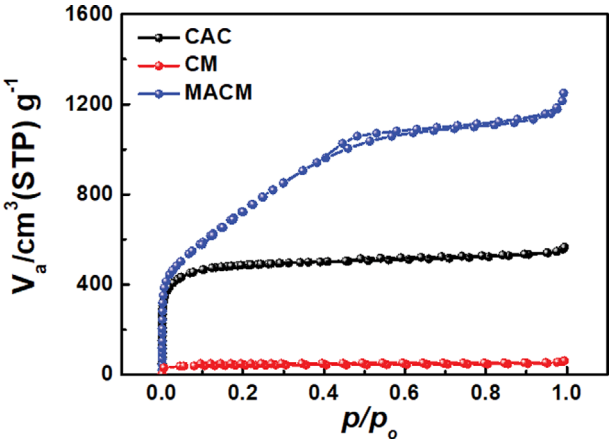

Fig. 4. BET result using N_2 adsorption/desorption of CAC, CM, and MACM.

providing one (pyridinic-N) or two (pyrrolic-N) charge carriers (electrons) to the carbon lattice. Moreover, the nitrogen dopant can offer the defect within the carbon structure, which can enhance the active site for energy storage. These positive effects can contribute to the high-rate energy-storage performance, enabling fast-charge-carrier transportation kinetics. Thus, MACM exhibits large specific surface area with the optimized mesoporous activated carbon morphology and high electrical conductivity owing to the N-doped carbon structure, which enhances the specific capacity and high-rate energy-storage capability, respectively [24].

Fig. 4 presents the BET analysis results for CAC, CM, and for characterizing the porous surface structure. The BET results reveal

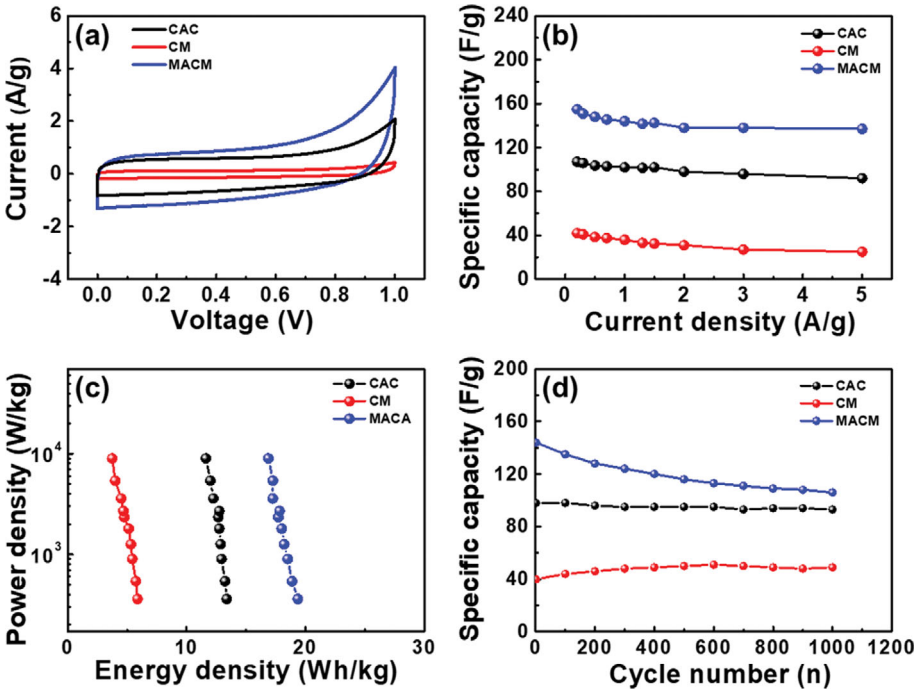

Fig. 5. (a) CV curves of CAC, CM, and MACM electrodes, (b) Specific capacity at a current density of 0.2-5 A/g, (c) Ragone plots of all the fabricated electrodes, and (d) result of cyclability test for 1,000 cycles at the fixed current density of 1 A/g.

that CAC is microporous and exhibits type I behavior, while CM appears to have a very low specific surface area owing to its bulk morphology without micropores. However, upon KOH activation, MACM shows type IV behavior at high N_2 pressures, corresponding to the mesoporous structure. Therefore, the optimized mesoporous activated carbon structure was successfully developed owing to the synergistic effects of mealworms' intrinsic amino acid and fatty acid profile paired with the KOH activation process. Moreover, MACM exhibited the largest specific surface area (2,470.5 m^2/g) in comparison with CAC (1,825.1 m^2/g) and CM (157.54 m^2/g). Owing to its superior specific surface area, MACM is also expected to exhibit a high specific capacity with sufficient charge adsorption/desorption sites.

To evaluate the electrochemical characteristics, cyclic voltammetry (CV) analyses were performed within the 0-1 V potential range and 10 mV/s scan rate. In Fig. 5(a), all electrodes exhibit rectangular CV data, implying the generation of electrostatic charging/discharging region [25]. As expected, among the MACM, CAC, and CM electrodes, the MACM electrode had the largest CV area, confirming its large charge storing area. Fig. S1 also demonstrates their electrical double-layer energy storage mechanism with liner galvanostatic charge/discharge curves, obtained from all the samples at a current density of 0.2-2.0 A/g. Fig. 5(b) shows the specific capacity obtained from CAC, CM, and MACM electrodes, which were acquired at a current density range of 0.2-5.0 A/g. The capacitance was calculated using the charge/discharge measurement. The specific capacity of the CAC, CM, and MACM electrodes was calculated to be 107, 42, and 154.8 F/g, respectively, at a 0.2 A/g. The high specific capacity of the MACM electrode at a low current density is caused by its large specific surface area that provides a sufficient electrical double-layer area [26]. Moreover, the MACM electrode showed the highest specific capacity of 137 F/g at a current density of 5 A/g in comparison with that of the CAC electrode (92 F/g) and CM electrode (30 F/g). This excellent high-rate energy storage capability is attributed to its well-developed mesopores, which leads to fast ion-diffusion kinetics. Fig. 5(c) shows the Ragone plots of all the electrodes. The MACM electrode shows a great energy density of 19.35-16.87 W h/kg. However, the CAC and CM electrodes exhibit low energy density (11.62-13.37 W h/kg for the CAC electrode and 5.87-3.75 W h/kg for the CM electrode). These results support the high energy-storage capability of the MACM electrode at both low and high current density. To evaluate the cyclability of the fabricated electrodes, long-term cyclability measurement was conducted for 1,000 cycles at a fixed current density of 1.0 A/g. The MACM electrode maintained the highest specific capacity of 106 F/g after 1,000 cycles compared to the CAC electrode (93 F/g) and CM electrode (49 F/g). However, a rapid decrease in specific capacity was observed at the MACM electrode, which is a chronic limitation of the biomass-derived activated carbon due to excessive surface functional groups. Therefore, additional research strategies are required to overcome this limitation, such as heteroatom doping and surface treatment. The Nyquist plots of all electrodes were constructed with the simulation data (applied circuit model was shown in Fig. S2) to investigate the kinetic properties and are shown in Fig. 6. The inclined line area reflects the ionic-diffusion ability through the interface region of

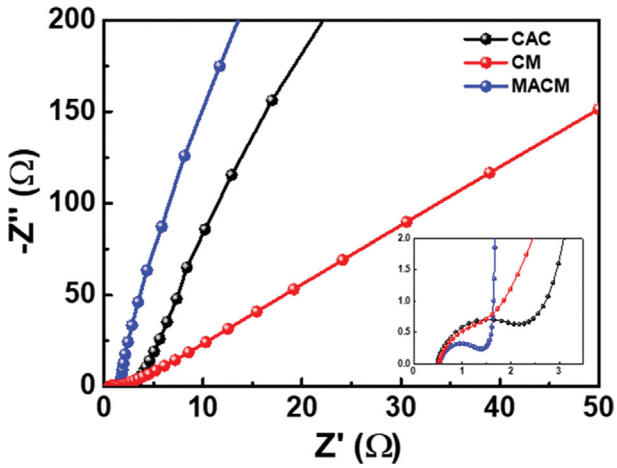

Fig. 6. Nyquist plots of CAC, CM, and MACM electrodes.

the electrode. Compared with the other electrodes, the MACM electrode produced the steepest incline in the plot owing to its well-developed mesoporous structure, which provides a favorable ion-diffusion path [27]. In addition, the semicircle region at high frequency confirms the electrical conductivity of the fabricated electrode (see inset of Fig. 6), where the MACM electrode possessed the smallest semicircle diameter. This result demonstrates the high electrical conductivity of MACM owing to its N-doped carbon structure [28].

In summary, mesoporous carbon with N-doped carbon structure was fabricated using protein-rich mealworm raw materials and KOH activation, which shows high energy-storage capability. The MACM electrode exhibited high specific capacity at both low and high current density. The maximum mesoporous morphology of the MACM sample was attributed to the synergistic effect of amino acid and fatty acid decomposition with KOH activation. The large specific surface area of MACM enables excellent specific capacity at a low current density. The N-doped carbon structure with mesoporous morphology yielded a high electrical conductivity with a shortened ion-transport pathway, offering a good high-rate capacity. Thus, based on the results, mesoporous activated carbon derived from mealworms could be a promising candidate for use as an active material in supercapacitors.

CONCLUSION

N-doped mesoporous activated carbon derived from a protein-rich mealworm raw material was successfully developed by harnessing the synergistic effect of amino acid and fatty acid decomposition and KOH activation during carbonization. MACM showed a superior specific surface area of 2,470.5 m^2/g, owing to a well-developed mesoporous morphology. The MACM electrode exhibited excellent electrochemical properties, including high specific capacities of 154.8 and 137 F/g at a low current density of 0.2 A/g and high current density of 5.0 A/g, respectively, and a capacity maintenance of 106 F/g after 1,000 cycles at 1.0 A/g. These performance enhancements were affected by the following factors: (1) large specific surface area owing to the optimized activation pro-

cess for a excellent specific capacity at a low current density and (2) a well-developed mesoporous morphology with an N-doped carbon structure for high capacity retention at a high current density. Thus, MACM electrodes could be an attractive substitute for conventional activated carbon in supercapacitor applications.

ACKNOWLEDGEMENTS

This study was supported by the Research Program funded by the SeoulTech (Seoul National University of Science and Technology).

CONFLICT OF INTEREST

The authors declare no conflict of interest.

SUPPORTING INFORMATION

Additional information as noted in the text. This information is available via the Internet at http://www.springer.com/chemistry/journal/11814.

REFERENCES

1. A. A. Kebede, T. Kalogiannis, J. V. Mierlo and M. Berecibar, *Renew. Sust. Energ. Rev.*, **159**, 112213 (2022).
2. J. Xiao, J. Han, C. Zhang, G. Ling, F. Kang and Q.-H. Yang, *Adv. Energy Mater.*, **12**, 2100775 (2022).
3. G. Chen, F. Wang, S. Wang, C. Ji, W. Wang, J. Dong and F. Gao, *Korean J. Chem. Eng.*, **38**, 46 (2021).
4. Y. Yang, E. G. Okonkwo, G. Huang, S. Xu, W. Sun and Y. He, *Energy Storage Mater.*, **36**, 186 (2021).
5. M. Singh, D. Zappa and E. Comini, *Int. J. Hydrog. Energy*, **46**, 27643 (2021).
6. K.-H Kim, J.-Y. Kim and H.-J. Ahn, *J. Ceram. Process. Res.*, **22**, 1 (2021).
7. S. Saini, P. Chand and A. Joshi, *J. Energy Storage*, **39**, 102646 (2021).
8. A. Jain, M. Ghosh, M. Krajewski, S. Kurungot and M. Michalska, *J. Energy Storage*, **34**, 102178 (2021).
9. M. Shaker, A. A. S. Ghazvini, W. Cao, R. Riahifar and Q. Ge, *New Carbon Mater.*, **36**, 546 (2021).
10. S. Rawat, R. K. Mishra and T. Bhaskar, *Chemosphere*, **286**, 131961 (2022).
11. Y. Liu, P. Liu, L. Li, S. Wang, Z. Pan, C. Song and T. Wang, *J. Electroanal. Chem.*, **903**, 115828 (2021).
12. K. Kanjana, P. Harding, T. Kwamman, W. Kingkam and T. Chutimasakul, *Biomass Bioenerg.*, **153**, 106206 (2021).
13. P. Manasa, S. Sambasivam and F. Ran, *J. Energy Storage*, **54**, 105290 (2022).
14. E. Lim, J. Chun, C. Jo and J. Hwang, *Korean J. Chem. Eng.*, **38**, 227 (2021).
15. V. Thirumal, K. Dhamodharan, R. Yuvakkumar, G. Ravi, B. Saravanakumar, M. Thambidurai, C. Dang and D. Velauthapillai, *Chemosphere*, **282**, 131033 (2021).
16. A. Wang, K. Sun, R. Xu, Y. Sun and J. Jiang, *J. Clean Prod.*, **283**, 125385 (2021).
17. S. Mancini, G. Sogari, S. E. Diaz, D. Menozzi, G. Paci and R. Moruzzo, *Foods*, **11**, 455 (2022).
18. K.-H. Kim, J. S. Lee and H.-J. Ahn, *Appl. Surf. Sci.*, **550**, 149266 (2021).
19. T. Liu, L. Zhang, W. You and J. Yu, *Small*, **14**, 1702407 (2018).
20. Y. Liu, Y. Wang, C. Shi, Y. Chen, D. Li, Z. He, C. Wang, L. Guo and J. Ma, *Carbon*, **165**, 129 (2020).
21. K.-H. Kim, D.-Y. Shin and H.-J. Ahn, *J. Ind. Eng. Chem.*, **84**, 393 (2020).
22. J. Kwon, K.-H. Kim, H.-J. Ahn and Y. Hwang, *J. Ceram. Process. Res.*, **22**, 186 (2021).
23. K.-H. Kim, W. Hu, H. S. Chang and H.-J. Ahn, *J. Alloy. Compd.*, **896**, 163148 (2021).
24. H.-G. Jo, K.-H. Kim and H.-J. Ahn, *Appl. Surf. Sci.*, **554**, 149594 (2021).
25. M. Gao, X. Wang, C. Xia, N. Song, Y. Ma, Q. Wang, T. Yang, S. Ge, C. Wu and S. S. Lam, *Korean J. Chem. Eng.*, **12**, 141 (2015).
26. M. A. Azam, N. S. N. Ramli, N. A. N. M. Nor and T. I. T. Nawi, *Int. J. Energy. Res.*, **45**, 8335 (2021).
27. D.-Y. Shin, J. S. Lee, B.-R. Koo and H.-J. Ahn, *Chem. Eng. J.*, **412**, 128547 (2021).
28. E. R.-Pinero, M. Cadek and F. Beguin, *Adv. Funct. Mater.*, **19**, 1032 (2009).

Supporting Information

N-doped mesoporous activated carbon derived from protein-rich biomass for energy storage applications

Kue-Ho Kim, Yun-Jae Song, and Hyo-Jin Ahn†

Department of Materials Science and Engineering, Seoul National University of Science and Technology, Seoul 01811, Korea
(*Received 15 September 2022 • Revised 12 October 2022 • Accepted 26 October 2022*)

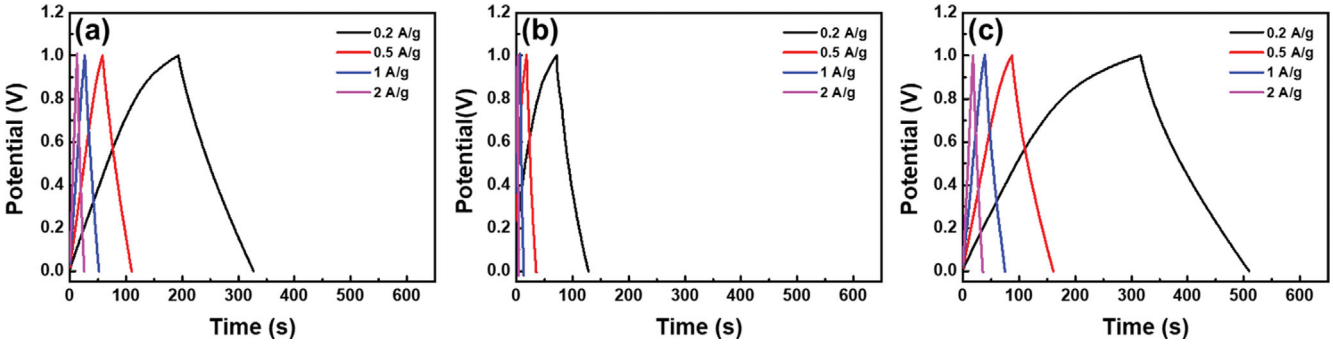

Fig. S1. GCD curves of (a) CAC, (b) CM, and (c) MACM, obtained at a current density of 0.2-2 A/g.

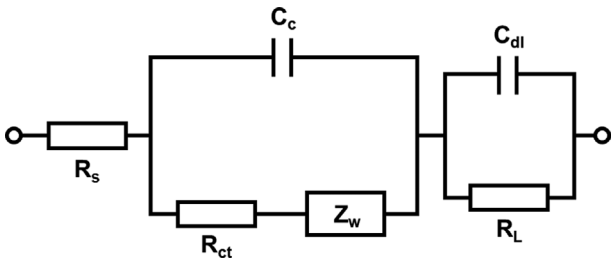

Fig. S2. Applied circuit model for EIS data simulation.